ELSEVIER

Thin Solid Films 352 (1999) 13–21

thin solid films

www.elsevier.nl/locate/tsf

Glow discharge plasma deposited hexafluoropropylene films: surface chemistry and interfacial materials properties

Michael D. Garrison[a, b], Reto Luginbühl[a], René M. Overney[c], Buddy D. Ratner[a, b, c,*]

[a]*University of Washington Engineered Biomaterials and the Department of Bioengineering, University of Washington, Seattle, WA 98195, USA*
[b]*National ESCA and Surface Analysis Center for Biomedical Problems, University of Washington, Seattle, WA 98195, USA*
[c]*Department of Chemical Engineering, University of Washington, Seattle, WA 98195, USA*

Received 19 August 1998; received in revised form 23 October 1998; accepted 10 November 1998

Abstract

Fluoropolymer films prepared by radio frequency glow discharge (RF-glow discharge) are of interest as biomaterials coatings. Previous studies focused on hexafluoroethane (C_2F_6, HFE) and tetrafluoroethylene (C_2F_4, TFE) as the monomer precursor have shown such surfaces to exhibit unique protein binding capabilities. In this study, slow, surface directed deposition of hexafluoropropylene (C_3F_6, HFP) films is shown to confer surface functional group presentation that promotes high protein retention. The surface chemistry is controllable over a range of values, and C_3F_6 films prepared by RF-glow discharge are smooth, homogeneous, and defect free. Surface patterns of the fluoropolymer can be created by direct or photolithographic techniques. Scanning probe microscopic analysis indicates a surface modulus in the range of $1.2 < E_{HFP} < 5.5$ GPa. These results are discussed in terms of the applicability of C_3F_6 films for coating biomaterials.

Keywords: Fluoropolymer films; RF-glow discharge; Scanning force microscopy; Electron spectroscopy for chemical analysis

1. Introduction

Fluorocarbon films deposited by radio-frequency glow discharge (RF-glow discharge, or 'plasma deposition') have found wide interest and application in the microelectronics, aerospace, automotive, and biomedical industries [1,2]. The RF-glow discharge method is a solvent free, room temperature process that allows for control of film thickness, texture, and surface chemistry through monomer selection and plasma reactor conditions. Fluoropolymer coatings produced by RF-glow discharge are attractive for industrial and research applications due to their smooth, conformal nature, low friction, low surface tension, and resistance to chemical attack. Such films are also pinhole free, crosslinked, and tightly bound to their substrate.

Films polymerized from perfluorinated monomers such as tetrafluoroethylene (C_2F_4, TFE), hexafluoroethane (C_2F_6, HFE) and perfluoropropane (C_3F_8, PFP) have generated interest as coatings to control biointeractions. RF-glow discharge fluoropolymer films from these monomers bind blood proteins tightly, resist platelet adhesion and activation when exposed to blood in vivo and have been proposed as a robust substrate for biomolecule immobilization in surface linked assays [3–6]. Recently, the plasma polymerization of hexafluoropropylene (C_3F_6, HFP) has been described in some detail [7–9]. The reactor conditions used in these studies supported gas-phase polymerization in addition to surface deposition. The resulting films appeared rough and displayed the incorporation of sub-micrometer particulates. Preliminary comparisons in our lab, using HFE, TFE, PFP, and HFP, indicated that smooth, defect free films could be produced by adjustment of the plasma conditions to promote surface polymerization [10].

The development of fluoropolymer coatings for biomaterials applications has focused on the non-thrombogenic and unique protein retention capabilities of these films. Multivariate analysis of HFE films has shown that the surface fluorine to carbon ratio (F/C), wettability, and composition of the film (CF_3/CF_2/CF/C–C ratios) as determined by electron spectroscopy for chemical analysis (ESCA) all play a role in determining the strength of protein retention [11]. This analysis showed that the CF_3 and CF_2 content, and the film F/C ratio, were parameters that positively correlated with increased retention of fibrinogen. Since it is known that monomers with high F/C ratios tend to etch surfaces

* Corresponding author. Department of Bioengineering, University of Washington, PO Box 351720, Seattle, WA 98195, USA Tel.: +1-206-685-1005; fax: +1-206-616-9763.
E-mail address: ratner@uweb.engr.washington.edu (B.D. Ratner)

0040-6090/99/$ - see front matter
PII: S0040-6090(98)01733-7

Table 1
Reactor conditions for HFP RFGD[a]

Power (W)	Time (min)				
	0.5	1	2	4	8
2	X				X
5	X	X	X	X	X
10					X
20					X
40	X				X

[a] flow rate = 2 sccm, reactor pressure = 150 mTorr: electrode area 0.01 m^2 (for one electrode), reactor cross sectional area = 86.59 cm^2: distance between electrodes = 15.24 cm.

rather than form polymerized films, it appears necessary to choose a monomer with low F/C, but perform the reaction under such conditions as to maximize the surface F/C in order to achieve maximal protein retention. Since the HFP monomer has a low fluorine to carbon ratio (F/C = 2, therefore good film forming properties), and a 1:1:1 ratio of CF_3/CF_2/CF functionality in the monomer, it should be possible to produce HFP films with similar high protein retention characteristics.

However, the mechanical properties of these coatings have received little attention. The exposure of the fluoropolymer coating to abrasion, wear, flexion, and chemical attack during device packaging, surgical handling, and in situ use can lead to delamination or degradation of the film quality. It is therefore desirable to have a coating that contains both the proper chemical and mechanical properties for good control of the desired biological response. A basic understanding of the relationship between the surface chemistry and the nanomechanical properties of RF-glow discharge films is essential for the development of robust biomedical coatings.

It is expected that the surface materials properties of RF-glow discharge deposited films can be controlled through adjustment of the process parameters. An emerging method for determining the contact mechanical properties of thin films exploits the scanning force microscope (SFM). SFM imaging allows for the surface morphology of the polymerized film to be determined in situ to nanometer resolution. SFM force curve spectroscopy allows for the determination of the film's viscoelastic response and surface modulus [12–15].

In this study, we investigated the surface chemical and material properties of RF-glow discharge deposited HFP fluorocarbon films. The quality of the films was ascertained by ESCA and SFM. ESCA provided evidence of successful surface modification, and the composition of surface chemistry present. Control over the surface chemistry was achieved by modification of the applied reactor power. SFM imaging and force curve spectroscopy assessed the surface morphology and nanomechanical behavior of the films. Smooth, highly crosslinked homogeneous films were produced, and the surface modulus measured. Patterned films were prepared by both direct and optical lithography.

2. Experimental

2.1. Substrate preparation

Cut (100) orientation silicon wafers (Silicon Quest Intl., Santa Clara, CA), were used as substrates for film deposition. Substrates were triply cleaned via sequential sonication in methylene chloride, acetone, and methanol (analytical grade, from commercial sources) dried in a stream of prepurified nitrogen, and immediately mounted in the plasma reactor.

2.2. Plasma deposition

Plasma deposition was conducted with a 13.56 MHz RF generator, capacitively coupled to symmetrical external electrodes via a matching network. The details of this reactor have been described elsewhere [11,16]. Hexafluoropropylene (PCR, Gainesville, FL), was used as the monomer precursor. C_3F_6 samples were reacted 'in the glow' (ITG) region between the coupling electrodes. Following deposition, all samples were 'annealed' in monomer flow for 5 min and brought to atmospheric pressure under argon. The samples were stored at room temperature in air. The matrix of deposition parameters, substrate, and monomer is contained in Table 1.

Using the theoretical framework advanced by Silverstein, we calculated the dimensionless plasma parameter E for our system according to

$$E = \frac{2W}{M_w(F_n)^3}\left(\frac{PA}{RT}\right)^2$$

where W is the applied power (Watts), M_w is the monomer molecular weight (g/mol), F_n is the molar flow rate (sccm), P is the steady state polymerization pressure (mTorr), A is the reactor cross sectional area (cm^2), R is the gas constant (J/mol-K), and T is the steady state temperature (K). A range of E values of $3.96e^{10} < E < 7.91e^{11}$ were obtained for our system using the conditions studied. This range is equal to or below the critical E_{ap} of $3.7e^{11}$ calculated by Silverstein for their reactor conditions [11]. Thus most of the plasma conditions used here can be described as 'energy starved'. Although substantial differences exist in the reactor geometry and substrate placement used in the previous studies and this work, it is nonetheless useful to note the plasma regime used here appears to be consistent with the hypotheses advanced by Silverstein, further illustrating the utility of such an approach.

2.3. Substrate patterning

A set of cut silicon wafers were prepared for photopatterning by sonicating in acetone for 5 min, followed by

Table 2
Compositional Analysis

Reactor power (W)	F (%)	C (%)	O (%)
2	58.9 ± 2.3	38.7 ± 2.6	2.4 ± 0.3
5	57.4 ± 1.4	41.5 ± 1.0	1.2 ± 0.5
10	56.5 ± 1.0	42.6 ± 0.8	1.0 ± 0.5
20	56.9 ± 0.9	41.7 ± 0.5	1.4 ± 0.5
40	57.8 ± 0.3	41.25 ± 0.5	1.0 ± 0.2

etching in concentrated hydrofluoric acid (Fisher) for 5 min. The samples were then immediately rinsed with copious amounts of distilled deionized water ($R = 18\text{M}\Omega$ US Filter Corp.) and dried in a stream of nitrogen. Positive photoresist (AZ1512, Shipley Inc.,) was applied by spin coating in a dual cycle manner (500 rev./min for 5 s, 3000 rev./min for 25 s), and then post-baked for 30 min at 90°C. The substrates were then mounted for contact proximity printing with a chromium mask containing two types of feature areas: (1) lines of 40 μm interspersed with 10 μm spaces and lines of 20 μm interspersed with 5 μm spaces, (2) regions of boxes 5,10,20 and 40 μm dimension. The photoresist was UV exposed for 60 s, then developed (Shipley AZ351 developer, 1:3 dilution in distilled deionized water) for 2 min with gentle agitation. The resulting patterned substrates were then rinsed in distilled deionized water, dried in a nitrogen stream, and mounted in the plasma reactor for fluoropolymer deposition as described above.

Following HFP deposition, the coated substrates were UV re-exposed (full field) for 60 s, and developed by sonication in a modified cocktail (1:1:3 AZ351/methanol/distilled deionized water) for 2 min. These fluoropolymer patterns were then rinsed in distilled deionized water and stored sealed in air.

2.4. Electron spectroscopy for chemical analysis (ESCA)

Electron spectroscopy for chemical analysis (ESCA) of the plasma deposited films was performed on a Surface Science Instrument (SSI, Mountain View, CA) S-Probe ESCA instrument, utilizing an aluminum K(1,2 monochromatized X-ray source and a hemispherical energy analyzer. This instrument permits the investigation of the outermost 20–100 Å of up to 1 mm^2 surface area of the sample at high (25 eV pass energy) or low (150 eV pass energy) resolution. Surface charging of the non-conducting films was minimized with an electron flood gun set at 5 eV. Typical pressures in the analysis chamber during spectral acquisition were 10^{-9} Torr. SSI data analysis software was used to calculate the elemental compositions from the peak areas in low-resolution spectra and peak fit the component peaks in the high-resolution spectral envelope. For this study, all spectra were recorded at a take-off angle of 55°. Spectral binding energies were referenced to the CF_2 peak assigned to 292 eV [17].

2.5. Scanning force microscopy (SFM)

Scanning force microscopy (SFM) was used to investigate and modify the plasma film morphology. A Nanoscope II SFM (Digital Instruments, Santa Barbara CA) was used for contact (constant force) mode imaging. 12 μm, 125 μm scanners, and triangular cantilevers with standard Si_3N_4 tips were used. Tip-sample forces were minimized (<10 nN), and scan rates held below 2.5 Hz. Normal forces were estimated from tip-sample force curve analysis, using force constants measured via the 'thermal noise' method [18]. Raw images were flattened to correct for non-linear curvature of the sample stage piezo tube response. Roughness values and surface feature dimensions were calculated using the software provided in the Nanoscope II control system. All Nanoscope SFM data was obtained under ambient conditions (~40–50% humidity, and 20–25°C).

Investigation of the material properties of the continuous and photolithographically patterned polymer films was performed using a Topometrix Explorer stand alone scanning force microscope (TMX 1010, Topometrix Corp., Santa Clara, CA). A 100 μm scanner, and 'non-contact' rectangular cantilevers with silicon tips were used. The spring constant of these cantilevers were calculated from the manufacturer's supplied cantilever dimensions and a measurement of the resonance frequency. The manufacturer's nominal values for tip radius was used. Contact mechanical measurements were performed in a dry nitrogen atmosphere (humidity $\lesssim$ 5%, 20–25°C).

3. Results and discussion

3.1. ESCA

3.1.1. Compositional analysis

ESCA analysis (Table 2) of all HFP RF glow discharge exposed surfaces exhibited predominant signals from fluorine (~58%) and carbon (~40%), indicating that a film had been deposited. Incorporation of contaminating species such as oxygen and nitrogen in the films were detected only to trace amounts (<1% oxygen; nitrogen not detected). In the case of films prepared at 2 W/30 s, a substrate signature was observed, indicating that these films were thinner than the 60 Å ESCA sampling depth.

3.1.2. Comparison of C1s envelope to monomer structure

High-resolution analysis of the HFP film C1s window indicated an overall envelope that mimicked the HFP monomer (Fig. 1). Although it appeared that some degree of the monomer structure was retained in these films ($CF_3/CF_2/CF$ ~1:1:1), the fluorine to carbon ratio (F/C) in the film was reduced ~40% relative to the monomer. This corresponds to an extraction on average of one to two fluorines per monomer unit during reaction initiation, and is consistent with reported values [7]. The CF_3 and CF_2 peaks appear to

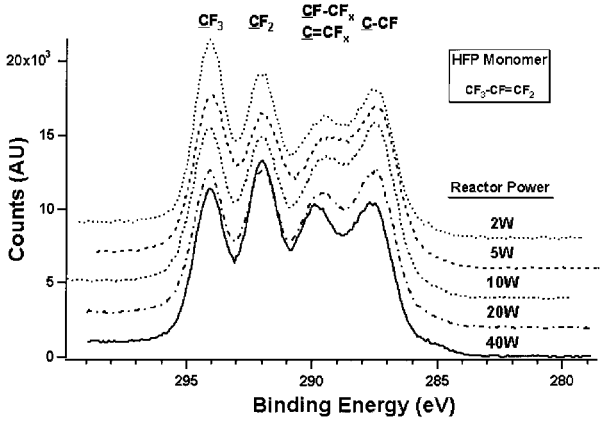

Fig. 1. High resolution C1s ESCA spectra of RFGD-HFP films as function of reactor power. Binding energies have been charge corrected by referencing the CF_2 peak to 292.0 eV. The vertical scaling has been offset for presentation purposes.

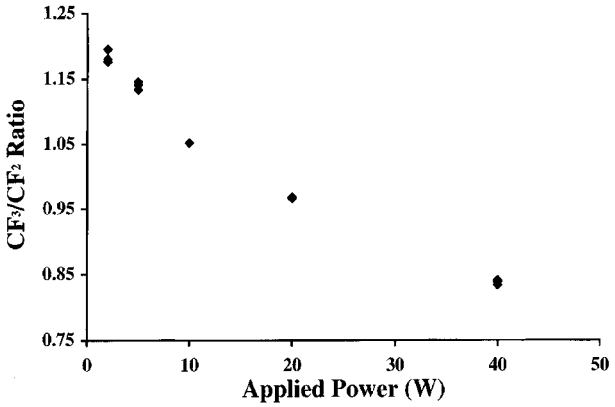

Fig. 3. Correlation of CF_3/CF_2 ratio to applied reactor power. Calculated from the high resolution spectra.

be well defined under all conditions tested. However, the CF–CF_x and C–CF_x peaks are broader and diffuse. Spectral broadening in this region occurs as a result of secondary shifts of the primary carbon due to adjacent neighbor binding conditions, overall environmental effects, or the presence of double bonds to the primary carbon [17]. The presence of a significant C–CF_x peak in all samples was an indication of a highly polymerized surface film. The C–CF_x peak was easily distinguishable from adventitious hydrocarbon located at 285 eV.

3.1.3. Control of fluorine to carbon ratio

Through analytical peak fitting of the C1s spectral window, a number of surface chemical properties could be calculated. The most consistent results were obtained by first performing an overall peak fit, allowing the full-widths at half maximum (FWHM) to be floating variables in the solution. Once this fit was obtained, the FWHM of the CF_2 peak was made equal to the CF_3 FWHM and both parameters fixed. The peak fit algorithm was then performed again, and the spectral areas obtained. Peak fitting in this manner allowed for separation of the broadening influence of the CF–CF_x peak from the CF_3 and CF_2 components [19]. The F/C of HFP ITG films was dependent upon the power applied to the reactor (Fig. 2). The range of F/C available through this procedure was small, ~1.35–1.5, or 10%. A slight decrease in F/C with increasing deposition time was also noted (Fig. 2 inset). This result suggests competitive etching processes that take place at the growing film surface which tend to remove F atoms from the film. Advantageously, the F/C ratio range of 1.35–1.50 lies exactly in the design regime that has been described for maximal protein retention [11]. The dynamic range of F/C achievable in this process appears to arise from spectral changes in the CF_3 component, and a shifting of the CF–CF_x peak, not from changes in the CF_2 peak. These phenomena are consistent with increased fragmentation of the monomer and fluorine extraction at high powers.

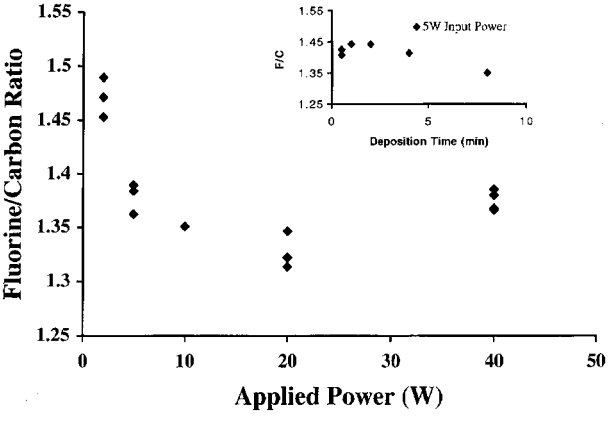

Fig. 2. Fluorine to carbon ratio (F/C) as function of applied reactor power. F/C = (3 × %CF_3 + 2 × %CF_2 + %CF)/Total as calculated from the high resolution C1s spectra. This analysis proved consistent with F/C calculated from the compositional spectra. Inset displays the F/C ratio as a function of deposition time for a constant power of 5 W.

3.1.4. Control of the CF_3/CF_2 ratio

In the HFP film, the CF_3 and CF_2 components are compositionally enhanced over the CF–CF_x and C–CF_x species. However, changing the reactor input power influenced the surface incorporation of CF_3 more so than the CF_2 component. This behavior was roughly linear (Fig. 3). At high powers (40 W) the CF_3 peak was reduced relative to the CF_2 peak, similar to that seen by Chen et al., and is consistent with enhanced fluorine extraction at high powers that drive the deposition/etching equilibrium towards an etching regime [7]. However, at low powers (e.g. 2 W), the CF_3 peak was dominant in the spectral window. This plasma regime is described as being 'energy starved'. The range of variation in CF_3/CF_2 was ~0.85–1.2 or 30%. Since previous work by Favia et al. has indicated that the CF_3 surface component is positively correlated with protein retention, the ability to enhance incorporation of the CF_3 species in the surface

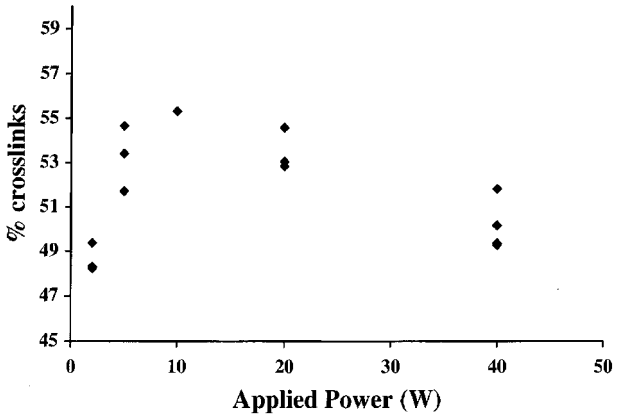

Fig. 4. Degree of crosslinking in HFP films as function of applied reactor power. Degree of crosslinking is calculated from the C1s spectra by: %crosslinks = ((%CF–CF_x+C–CF_x)/Total).

film represents a significant advantage of RF-glow discharge in the energy starved regime.

3.1.5. Shifting of CF peak

A second effect of increasing the reactor power is also noted. The CF–CF_x peak shape becomes more prominently resolved and shifts to higher binding energy relative to the C–CF_x peak (Fig. 2, 20 and 40 W films). The shift in the peak maximum is ~1 eV, which might be a secondary effect of the CF_3 component reduction, or caused by the same reaction mechanism. There was no peak shift noted as a function of reaction time. The character of the CF–CF_x peak at low powers was similar to that found in TFE, but at high powers had shifted in binding energy to a peak position similar to that found in PFP [10]. TFE monomer contains a primary double bond (CF_2=CF_2), while PFP monomer has no double bond character (CF_3–CF_2–CF_3). Since the plasma conditions used at low powers are energy starved, it is expected that greater retention of the monomer structure would occur in the surface film. The lowest energy bond to be broken in the HFP monomer is the C–C bond (80 kcal/mol) between the CF and CF_3 moieties [2]. The C=C double bond (142 kcal/mol) is nearly twice as energetic, and may be more likely to participate in the surface polymerization reaction at low powers. Therefore, the CF–CF_x peak shifting seen in HFP as a function of reactor power is supportive evidence for the retention / elimination of double bond character in the surface films. This data supports the assumption of having CF=CF_2 bonds with a binding energy assignment in the region of 289 eV.

3.1.6. Degree of crosslinking

NEXAFS studies have shown that 'in the glow' RF glow discharge polymerized TFE films are highly disordered due to random branching and crosslinking [20]. The strong contributions in the HFP C1s spectra of the CF–CF_x and C–CF_x peaks indicate a similarly high degree of branching and crosslinking in the HFP surface film. The CF–CF_x species represents branching sites in the polymer. However, the presence of residual double bond character (which would be a chain propagating species) located in this binding energy window makes resolution of the degree of branching difficult. If we consider only the percentage contribution of the C–CF_x peak, then ~30% of the carbon atoms are involved in crosslinking. Assuming the crosslinks are randomly distributed in the polymer, an average run of linear polymer would be approximately 4 carbons in length: $(CF_n)_4$, $n = 1, 2$. As calculated, the loss of CF_3 should not affect this parameter, although the mechanism of CF_3 loss may influence the crosslinking behavior. The range of crosslink density (including branching) was 45–55%, with minima occurring at 2 and 40 W, and maxima occurring at 10 and 20 W (Fig. 4) This behavior is consistent with loss of monomer structure due to increased etching processes.

3.2. SFM

3.2.1. Roughness and morphology

Contact mode SFM image analysis of the HFP films prepared by RF glow discharge revealed surfaces that were pinhole free, and very smooth. (Fig. 5) The RMS roughness of these films varied from 4–20 Å over image sizes of 9–100 μm^2. Increasing power or deposition time appeared to have no effect on the film morphology or roughness. Separation of the film into islands as seen in C_2F_6 'afterglow' films was not observed, even for films <60 Å [11]. However, the morphology of the surface did suggest surface growth kinetics consistent with island formation. These islands appear to be less than 50 nm in diameter. Features such as sub-micrometer spheres noted by Chen et al., were not observed in the conditions studied here, although these particulates have been detected when prepared at 100 W applied power [7,8]. Since our plasma

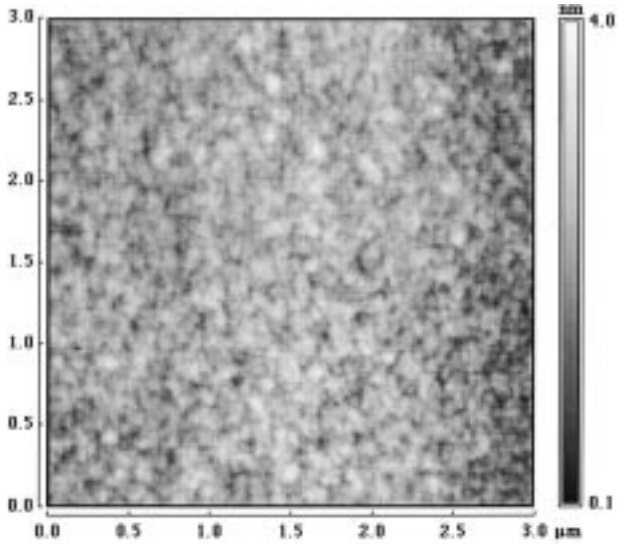

Fig. 5. Contact mode SFM image of 20 W/8 min film. RMS roughness for this image is 4.5 Å.

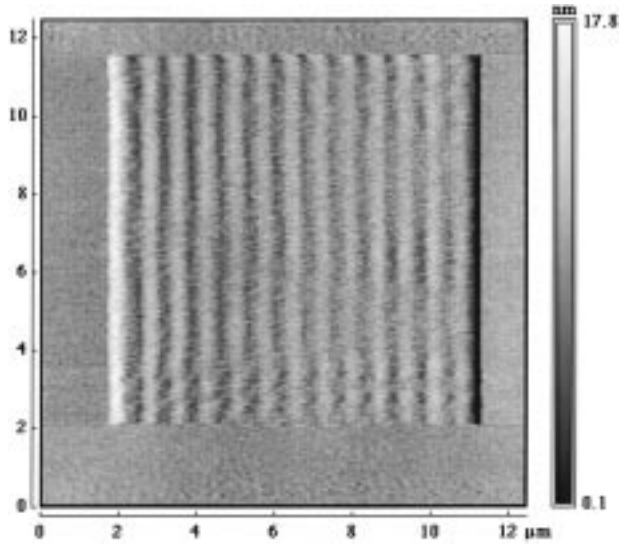

Fig. 6. Direct surface patterning. Wave formation due to tip-sample wear is induced as a function of surface velocity. 5 W/8 min film.

was energy starved, the deposition rate was decreased to allow for smooth, continuous deposition, with reduced competitive etching effects at the surface. Given the smooth nature of these films coupled with the tight binding properties, they are attractive substrates for the investigation of protein structure.

3.2.2. Modification of surface structure

It was noted that prolonged imaging of the HFP surfaces at increased normal loads could disrupt the films and induce surface features. Selective modification of the surfaces was possible by choosing a desired scan area, increasing the tip loading, and increasing the surface velocity. Two general types of behavior were found.

(1) At large scan areas and moderate applied loads, the films tended to ripple (Fig. 6), perpendicular to the scan direction. This type of wave induction has been reported in many polymeric surface film systems, and is thought to be a manifestation of 'Schallmach waves' [21–24]. Formation in the soft fluoropolymer films occurs in response to the relatively soft film being moved under the hard SFM tip. The periodicity of the ripples induced in the HFP appeared to be primarily a function of the surface velocity, although this relationship was not studied in depth. The dependence on surface velocity was not described in the induction of ripples in gelatin films [24]. It is possible that the strong adhesion of the HFP films to the SFM tip plays an important role in this process.

(2) At small scan sizes (<5 μm) high surface velocities ($\sim$ 40 μm/s), and large tip loading values (>60 nN), the films tended to disrupt and wear, revealing an underlayer that resisted further abrasion (Fig. 7). It is felt that this underlayer is the film substrate. This behavior was common to all film types, but the normal force required to disrupt the film increased with decreasing F/C ratio. The film resistance to deformation appeared to be a function of the degree of crosslinking, although it is also possible that differences in the surface chemistry alter the lateral forces acting in the system resulting in differential relative wear. Further studies are required to clarify this point. Direct disruption of the films provided the means to measure the film thickness and thereby calculate the growth rate of the overlayer. Fig. 7 displays a set of holes created by SFM lithography. At high powers and 8 min deposition time, the 10 W films required >8 h scanning to reach the substrate. In the case of the 20 and 40 W (8 min) films, the substrate was not completely exposed even after 16 h of increased load scanning ($k_{cant} = 0.35$ N/m). The 8 min 40 W films were especially resistant, but the 30 s 40 W films could be etched to the substrate. Thus, two conclusions could be drawn. First, the increased tip loading needed to disrupt the films was probably due to changes in the tip-sample interaction, and the bulk structure of the HFP films. This was expected in light of the changes in F/C ratio, and degree of crosslinking as determined by ESCA. Secondly, the difficulty in removing surface film from thicker coatings was probably not due to changes in the HFP structure, but rather a contact pressure effect. As the tip penetrated deeper into the film, the contact area increased, thus reducing the effective force/unit area on the film. The reduced force/unit area decreased the rate of wear, similar to the effects seen in Fig. 7.

3.2.3. Patterned films

Since the higher power films were not easily etchable by direct SFM lithography, a set of photolithographically patterned samples were coated with HFP, developed and imaged. Fig. 8 shows an SFM topograph of a patterned HFP film in a region of 20 μm boxes. The surface topography reveals raised regions of fluoropolymer, separated by exposed silicon. Film thicknesses were calculated from the line scan and histogram analyses performed perpendicular

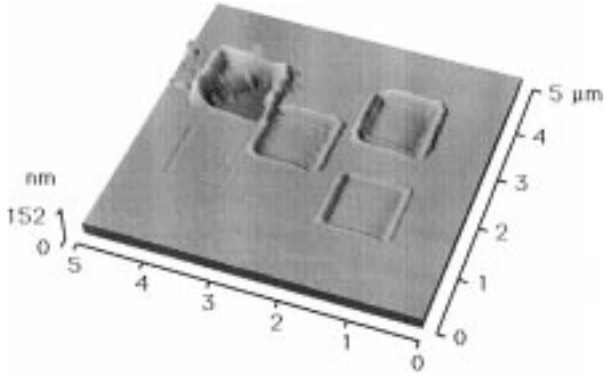

Fig. 7. Direct surface patterning. Direct etching of a 5 W/8 min film, as a function of applied load and wear time. The boxes were etched with the following conditions: upper left (65 nN/7 min), upper right (65 nN/3 min), lower right (38 N/1 min), lower left (16 nN/1 min), and center (65 nN/1 min).

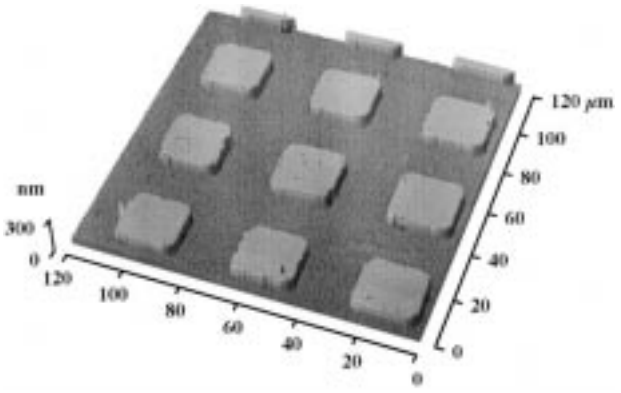

Fig. 8. Contact mode SFM of photolithographically patterned C_3F_6 on silicon. Image shows a grid pattern of 20 mm squares. Patterns with lines and squares have been prepared in the feature size range of 5–40 μm.

across the patterns. Fig. 9 shows the effect of power and deposition time on the growth of the fluoropolymers. There was good agreement in the film thickness as a function of reactor power measured from the photolithographically patterned films and the films patterned by SFM lithography. A linear curve fit to the initial portion of the curve gives a growth rate of 22.2 Å/W-min. Assuming a density of 2.21 g/cm^3, this value corresponds to a deposition rate (R_d) of 0.5 μg/cm^2-W-min, which is a factor of ~300 less than that used by Chen et al. [7]. The markedly reduced deposition rate is consistent with the surface dominated reaction parameters used to obtain the smooth featureless films. It should be noted that in order to remove the photoresist, an acetone stripping procedure was initially attempted. The HFP films were delaminated by this treatment, as described by Chen et al. This behavior is interesting since one might expect the solubility parameter of HFP to be similar to PTFE (γ_{PTFE} = 12.7 MPa$^{1/2}$, $\gamma_{acetone}$ = 19.5 MPa$^{1/2}$) [25]. However, the HFP films do not display the crystalline structure of PTFE which tends to dominate the solubility behavior. Delamination was not observed when the films were immersed in ethanol (γ_{EtOH} = 26.7 MPa$^{1/2}$) or methanol (γ_{MeOH} = 29.7 MPa$^{1/2}$). It was also noted that the surfaces appeared to degrade

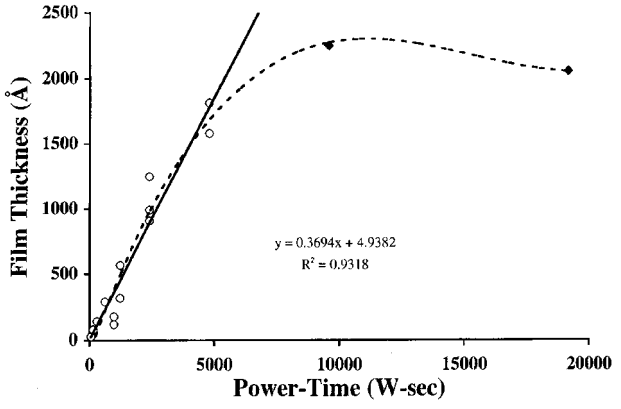

Fig. 9. Film thickness as function of deposition time and reactor power. The linear fit to the data excludes the 20 W/8 min and 40 W/8 min films (◆).

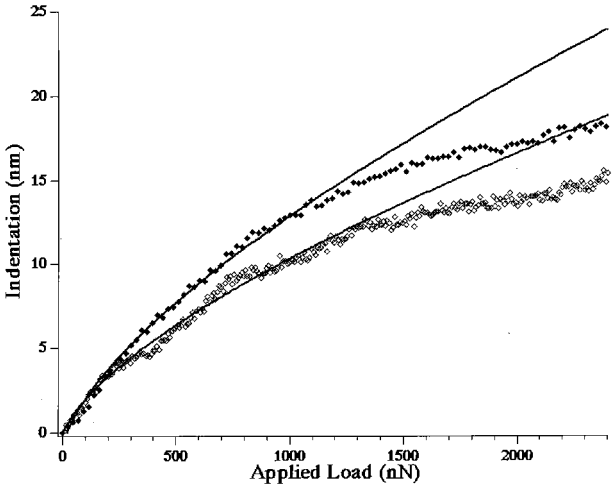

Fig. 10. Indentation versus load response of an HFP 5 W/8 min film. Curve fit to initial regime (load $<$ 1200 nN) using a Hertz model ($F = (4/3) \times (E/1 - \nu^2)) \times R^{1/2} \times \delta^{3/2}$), where F is the loading force, E is the Young's modulus, ν is Poisson's ratio (assumed to be 0.5), R is the tip radius, and δ is the indentation into the film. δ is calculated from the difference of the sample response to the response on silicon. Two representative data sets are shown for the purpose of illustrating the degree of variation observed in the film response.
$E_{(\blacklozenge)}$=2.4 GPa, χ^2=7.3; $E_{(\diamond)}$=3.6 GPa, χ^2=20.5 (assuming R=20 nm).

slightly through the development procedure. Pinholes and defect sites, not seen in the unpatterened films, were revealed within the HFP lanes. In some cases delamination of the HFP lanes was observed. We feel strongly that refinement of the photolithography and development protocols will eliminate these deleterious effects.

3.2.4. Surface modulus

Point force spectroscopy of the HFP films revealed significant differences compared to the silicon controls. Force versus displacement curves on the HFP surface displayed a weak repulsive force near the contact point upon approach, and a large adhesive force upon retraction. The slope of the constant compliance region on the fluoropolymer films was non-linear. Using the method described by Radmacher et al., an indentation versus applied load curve was developed [12,15]. This curve displayed two regimes. At low loads ($\backsim <$ 1200 nN) there appeared to be a power law dependent behavior to the indentation (Fig. 10). At high loads ($\backsim \geq$ 1200 nN), the deflection response approached that of the silicon reference substrate (E_{SiO_x} = 151 GPa), [26], due to the polymer film compression and resulting influence of the stiff underlayer. This behavior is consistent with the elastic response of thin films under static force curve analysis [15]. Curve fitting the indentation curve using the Hertzian contact mechanical model and assuming a range of tip radii, ($60 \geq R \geq 5$ nm) the surface modulus could be estimated as $1.2 \pm 0.5 < E_{HFP} < 5.5 \pm 1.8$ GPa (average of 10

force versus indentation plots, each force curve an average of 5 individual force curves.

Uncertainty in the modulus value at small indentations (<30 nm) has been shown for a range of polymers, including polystyrene ($E = 1$–3 GPa)[14]. It has also been shown that in this modulus range our commercially available cantilevers ($k_{cant} = 33$ N/m) may not be adequate to resolve small modulus differences due to small indentations [13]. Some variation in the initial response at low loads in the force curves was noted during the indentation experiments, possibly due to alterations in the tip properties (see below). This variation often resulted in poor residual values when fit to the Hertzian model. As a result of these uncertainties, we view the surface modulus value calculated here as an order of magnitude estimate, and did not attempt to make comparisons between films prepared at different powers. Even so, the modulus value is consistent with the observed wear behavior of the polymer films as described above. Furthermore, the E_{HFP} calculated here is consistent with that reported for PTFE, and other fluorine containing polymers. ($E_{PTFE} \approx 0.5$ GPa) [27].

In the retraction trace of the force curves on the silicon surface, the snap-off was found to occur very near the point of contact. This indicates a lack of adhesive force between the tip and the sample when examined under dry nitrogen. On the fluoropolymer however, a large snap-off adhesive force was always measured. This behavior indicates a high affinity of the HFP polymer for the tip surface. Since the HFP films exhibit strong affinity for the hydrophobic silicon substrate in polar solvents, and resist delamination under sonicating conditions, it is reasonable to assume that the HFP surface would also have strong affinity for the silicon or silicon nitride SFM tip surface. The magnitude of the measured adhesive force correlated to the applied load. The pull-off was always singular however, indicating that a unique separation event occurs. Multiple polymer strands do not appear to adhere to the tip and break separately. The adhesive behavior was reversible when performed on side by side silicon lanes using the patterned HFP samples [16]. However, it should be noted that following extended imaging or force curve analysis, the SFM tips occasionally displayed anomalous behavior when tested on clean silicon or mica. We attribute this phenomenon to a 'staining' of the probe tip by the fluoropolymer (unpublished results). It is probable in these cases that some material from the film adhered very strongly to the tip during scanning and spectroscopy, thereby contaminating the tip surface. Due to the variation observed in the indentation method of calculating the modulus, and the strong adhesion forces measured on the HFP, we are actively pursuing alternate strategies for mapping the surface nanochemical properties. Promising avenues include force curve spectroscopic mapping using the pulsed force 'mode' and force modulation microscopy [16,28].

The results of this study indicate that smooth, continuous, highly adherent fluoropolymer films can be produced by RFGD plasma deposition using HFP as the monomer source. The film surface chemistry as reflected by the F/C and CF_3 content is such that these surfaces should display tenacious protein binding character. The surface chemistry is controllable through alteration of the reactor power, while the thickness may be controlled by the reaction time. The HFP films are crosslinked, and display a surface modulus in the range of $1.2 < E_{HFP} < 5.5$ GPa. Patterning of the fluoropolymers is possible by direct or photolithographic techniques. Patternable surfaces with areas of different biological adhesiveness represent novel probes of cell and biological function [29], and may eventually be useful for implant biomaterials. This work describes new methods for both controlling protein adhesiveness (via surface chemistry) and for patterning such surfaces. Biological and biomedical applications are currently being explored.

Acknowledgements

This work was supported by: UWEB (University of Washington Engineered Biomaterials, NSF grant EEC 9529161), the National ESCA and Surface Analysis Center for Biomedical Problems (NESAC/BIO NIH NCRR grant RR01296), the University of Washington Center for Nanotechnology, and the Whitaker Foundation. M. Garrison was also supported through a US Department of Education GAANN Fellowship and the University of Washington Department of Bioengineering. R. Luginbühl is supported by a Swiss National Science Fellowship. Dr. Overney is supported in part by the Royal Research Foundation (UW] and the Exxon Educational Foundation. Special thanks to Dave Castner, Winston Ciridon, Andreas Goessel, and Steve Golledge for their assistance and stimulating discussions.

References

[1] H. Yasuda, Plasma Polymerization, Academic Press, Orlando, FL, 1985 pp. 432.
[2] R. d'Agostino, F. Camarossa, F. Fracassi, F. Illuzzi, in: R. d'Agostino (Ed.), Plasma Deposition, Treatment, and Etching of Polymers, Academic Press, Boston, MA, 1990, pp. 95.
[3] D. Kiaei, A.S. Hoffman, T.A. Horbett, J. Biomater. Sci. Polym. Ed. 4 (1992) 35.
[4] D. Kiaei, A.S. Hoffman, S.R. Hanson, J. Biomed. Mater. Res. 26 (1992) 357.
[5] D. Kiaei, A.S. Hoffman, T.A. Horbett, K.R. Lew, J. Biomed. Mater. Res. 29 (1995) 729.
[6] Y. Haque, B.D. Ratner, J. Polym. Sci. B. 26 (1988) 1237.
[7] R. Chen, V. Gorelik, M.S. Silverstein, J. Appl. Polym. Sci. 56 (1995) 615.
[8] R. Chen, M.S. Silverstein, J. Polym. Sci. A 34 (1996) 207.
[9] M.S. Silverstein, R. Chen, O. Kesler, Polym. Eng. Sci. 36 (1996) 2542.
[10] M.D. Garrison, B.D. Ratner, ACS Polymer Preprints 38 (1997) 989.
[11] P. Favia, V.H. Perez-Luna, T. Boland, D.G. Castner, B.D. Ratner, Plasmas and Polymer 1 (1996) 299.
[12] M. Radmacher, M. Fritz, P.K. Hansma, Biophys. J. 69 (1995) 264.

[13] M.R. Vanlandingham, S.H. McKnight, G.R. Palmese, R.F. Eduljee, J.W. Gillespie Jr, R.L. McCulough, J. Mater. Sci. Lett. 16 (1997) 117.
[14] S.A. Chizhik, Z. Huang, V.V. Gorbunov, N.K. Myshkin, V.V. Tsukruk, Langmuir 14 (1998) 2606.
[15] J. Domke, M. Radmacher, Langmuir 14 (1998) 3320.
[16] R. Luginbuhl, M.D. Garrison, R.M. Overney, L. Weiss, H. Schieferdecker, S. Hild, B.D. Ratner, in: D. Castner (Ed.), Proceedings in ACS Polymer Series, 1998.
[17] A. Dilks, in: C.R. Brundle, A.D. Baker (Eds.), Electron Spectroscopy Theory, Techniques, and Applications, Academic Press, New York, 1981, pp. 277.
[18] J.L. Hutter, J. Bechtoefer, Rev. Sci. Instrum 64 (1993) 1868.
[19] A. Dilks, Characterisation of Polymers by ESCA, Applied Science, Essex, UK, 1986.
[20] D.G. Castner, K.B. Lewis, D.A. Fischer, B.D. Ratner, J.L. Gland, Langmuir 9 (1993) 537.
[21] A. Schallmach, Wear 17 (1971) 301.
[22] O.M. Leung, M.C. Goh, Science 255 (1992) 64.
[23] S.W. Hui, R. Viswanathan, J.A. Zasadzinski, J.N. Israelachvili, Biophys. J. 68 (1995) 171.
[24] M. Radmacher, P.K. Hansma, ACS Polymer Preprints 37 (1996) 587.
[25] F. Rodriguez, Principles of Polymer Systems, Vol. 1, Hemisphere, New York, 1989, pp. 29–34.
[26] M. Ohring, The Materials Science of Thin Films, Academic Press, New York, 1992.
[27] J.B. Park, Biomaterials Science and Engineering, Vol. 1, Plenum Press, New York, 1987, pp. 288–290.
[28] R. Luginbuhl, M.D. Garrison, R. Overney, B.D. Ratner, (1999) in preparation.
[29] X. Chen, M.C. Davies, C.J. Roberts, S.J.B. Tendler, P.M. Williams, J. Davies, A.C. Dawkes, J.C. Edwards, Langmuir 13 (1997) 4106.